A TECHNICAL NOTE ON THE UNCERTAINTIES OF THE CHEN CORRELATION FOR THE BOILING HEAT TRANSFER COEFFICIENT AT SATURATED FLOW

by

Electra D. POULOPOULOU and Nick P. PETROPOULOS*

Nuclear Engineering Laboratory, School of Mechanical Engineering,
National Technical University of Athens, Athens, Greece

Technical paper
https://doi.org/10.2298/NTRP2402160P

The so-called *Chen correlation* for the boiling heat transfer coefficient at saturated flow has been, since 1966, the year of its publication, largely cited as one of the most successful of its kind. As well known, it is based on adding terms respective to heat transfer in the liquid part and heat transfer in the steam part. The respective formulae incorporate both the Reynolds number factor *F* and the suppression factor *S*. At the time, Chen accepted *F* and *S* to be derived graphically. Nevertheless, and mainly for computational purposes, several equations have been proposed approximating these two factors. These equations have been reviewed for accuracy and typos and are now widely accepted. However, there has not been any attempt to associate the results of the Chen correlation with the expected uncertainty. The objective of this short report is to process the Chen correlation in terms of its uncertainty based on the uncertainty of factors *F* and *S*. The uncertainties of *F* and *S* were derived digitally from the graphs of *F* and *S* in the original work of Chen of 1966. Following digitization the uncertainty data were processed to provide uncertainty formulae in polynomial form. It was accepted that the uncertainty level of F and S was $k = 1$.

Key words: Chen correlation, flow boiling at saturation, heat transfer coefficient, Reynolds number factor, suppression factor

INTRODUCTION

The Chen correlation for the heat transfer coefficient of saturated flow boiling, as in [1, 2], is one of the most widely used in flow boiling heat transfer problems. As per today's (2024) available data it has been cited about 3000 times (as per the Google Scholar data in early 2024). According to this correlation, two-phase flow boiling heat transfer coefficient *h* could be described by the heat transfer of forced convection (fc) within the saturated liquid and the heat transfer of saturated nucleate boiling (nb). The two components act in an additive manner and their weight in the sum could be accounted using the Reynolds number factor *F* and the suppression factor *S*. Therefore, it is

$$h = F h_{\mathrm{fc}} + S\, h_{\mathrm{nb}} \tag{1}$$

Chen [2] successfully suggested that the hfc component could be described using the Dittus and Boelter equation [3].

* Corresponding author, e-mail: npetr@mail.ntua.gr

Further, he successfully accepted that the hnb could be determined by the Forster and Zuber equation [4]. The details of both equations are available in their original publications and the successive publications mentioning the Chen correlation. However, the h_{fc} component is a function of a liquid Reynolds number $\mathrm{Re_l}$ as provided by the formula

$$\mathrm{Re_l} = \frac{(1-x)GD_{\mathrm{h}}}{\mu_{\mathrm{l}}} \tag{2}$$

where x is the quality of the steam, G [kgm^{-2}s^{-1}] – the mass flux, D_{h} [m] – the hydraulic diameter, and μ_{l} [Pas^{-1}] – the dynamic viscosity of the liquid.

Chen [2] further suggested that there exist graphical functions for the Reynolds number factor *F*, fig. 1 and the suppression factor *S*, fig. 2. The graphs in figs. 1 and 2 were derived heuristically based on numerous experimental data. Figure 1 is a plot of *F vs* the reciprocal of the Martinelli parameter $1/X_{\mathrm{tt}}$ calculated by

$$X_{\mathrm{tt}} = \left(\frac{1-x}{x}\right)^{0.9}\left(\frac{\rho_{\mathrm{g}}}{\rho_{\mathrm{l}}}\right)^{0.5}\left(\frac{\mu_{\mathrm{l}}}{\mu_{\mathrm{g}}}\right)^{0.1} \tag{3}$$

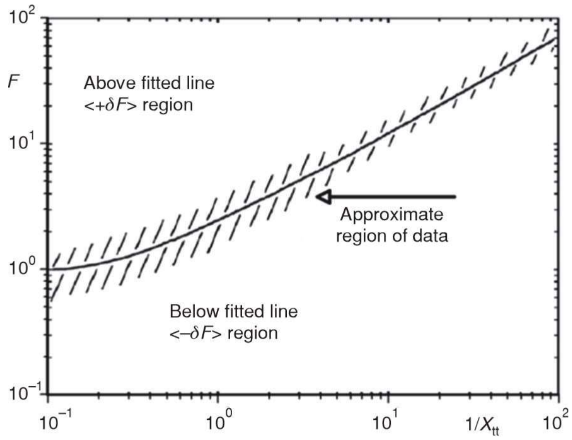

Figure 1. Reynolds number factor, *F* [5]

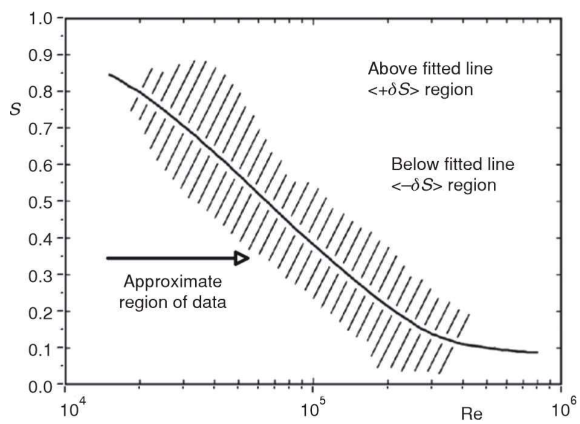

Figure 2. Suppression factor, *S* [5]

where ρ [kgm^{-3}] is the density, g – the gaseous phase, and l – the liquid phase

Figure 2 is a plot of S *vs.* the effective two-phase Reynolds number. This effective Reynolds is a function of F as in

$$\mathrm{Re} = \mathrm{Re}_1\, F^{1.25} \tag{4}$$

In figs. 1 and 2 the curves are graphical best fits for F and S respectively, while the shaded areas account for the respective deviation <+δF>, <–δF> and <+δS>, <–δS> around the fitting functions.

Chen [2] did not prepare any equations for these best fits or deviations. However, and for obvious reasons, others have proposed in succession several such equations as best fits for F and S. A different Chen and Fang [5] has presented and critically reviewed all up to the then-existing expressions for F and S and compared these expressions with the original graphs in [2]. It could be said, and this is accepted in this study, that the most accurate expression for F could be

$$F = \begin{cases} 2.35\,(1/X_{\mathrm{tt}} + 0.213)\,0.736, & \text{if } 1/X_{\mathrm{tt}} > 0.1 \\ 1, & \text{if } 1/X_{\mathrm{tt}} \le 0.1 \end{cases} \tag{5}$$

i.e., the one proposed and agreed in [6-16]. Further discussion on the accuracy of this expression can be found in [5].

It could be said also, and this is accepted in this study as well, that the most accurate expression for S could be the one proposed in [13]

$$S = \begin{cases} 1/\,(1+0.12\,\mathrm{Re}_{\mathrm{TP}}^{1.14}), & \text{for } \mathrm{Re}_{\mathrm{TP}} < 32.5, \\ 1/\,(1+0.42\,\mathrm{Re}_{\mathrm{TP}}^{0.78}), & \text{for } 32.5 \le \mathrm{Re}_{\mathrm{TP}} \le 70, \\ 0.0797\mathrm{e}^{(1-\mathrm{Re}_{\mathrm{TP}}/70)}, & \text{for } \mathrm{Re}_{\mathrm{TP}} > 70 \end{cases} \tag{6}$$

where $\mathrm{Re}_{\mathrm{TP}}$ is the effective two-phase Reynolds number as in

$$\mathrm{Re}_{\mathrm{TP}} = 10^{-4} \cdot \mathrm{Re}_1\, F^{1.25} \tag{7}$$

Further discussion on the accuracy of this expression could be also found in [5]. However, up to now (2024) it seems that nobody would care to effectively address the precision of the graphs and the provided expressions. Therefore, this short report attempts to examine this problem.

METHODS

As well known in the respective theory, for a function q of several variables $x, y, \ldots, z$, which is computed as $q(x, \ldots, z)$, $x, y, \ldots, z$ could be measured uncertainties $\delta x, \ldots, \delta z$. These uncertainties, as per [17], may include both Type A and Type B components and are used to quantify the uncertainty of q

$$\delta q = \sqrt{\left(\frac{\partial q}{\partial x}\delta x\right)^2 + \ldots + \left(\frac{\partial q}{\partial z}\delta z\right)^2} \tag{8}$$

Equation (8) stands if the measurement of x (or y or z, *etc.*) has the form $x_{\mathrm{best}} \pm \delta x$. Then the best estimate of q is $q_{\mathrm{best}} = q(x_{\mathrm{best}}, y_{\mathrm{best}}, etc.)$. Since, for the examined case, F and S have been estimated by several contributors using various methods, there is trust that the relevant errors are not related. Applying eq. (8) to eq. (1) at least part of the uncertainty of the heat transfer coefficient could be obtained as a function of the uncertainties of quantities F and S. This uncertainty could be accepted as total uncertainty under the assumption that there is no significant uncertainty contribution from other parameters involved in the calculation. Therefore

$$\delta h = \sqrt{(h_{\mathrm{fc}}\delta F)^2 + \ldots + (h_{\mathrm{nb}}\delta S)^2} \tag{9}$$

with unknowns δF and δS, for which there exist only graphical representations and no mathematical formulae.

In this work, the uncertainty ranges of F and S have been digitized from the graphs of figs. 1 and 2. Then, the data for <δF> and <δS> derived from the digitization were fitted to polynomial correlations as functions. In the case of F, <$\pm\delta F$> was calculated as a function of F and as a function of $1/X_{\mathrm{tt}}$. In the case of S, <$\pm\delta S$> was calculated as a function of S and as a function of $\mathrm{Re}_{\mathrm{TP}}$.

It goes without saying that there were no weights assigned for different values of $\langle \pm\delta F \rangle$ and $\langle \pm\delta S \rangle$ since such weights are unknown. It is understandable from fig. 1 that for each F and each $1/X_{tt}$, there would be two polynomial fittings, one for $\langle +\delta F \rangle$ and one for $\langle -\delta F \rangle$. In the same way, it is derived from fig. 2 that for each S and each Re_{TP}, there would be two polynomial fittings, one for $\langle \pm\delta S \rangle$ and one for $\langle -\delta S \rangle$. Due to the obvious shapes of $\langle +\delta F \rangle$, $\langle -\delta F \rangle$, $\langle +\delta S \rangle$ and $\langle -\delta S \rangle$ the polynomials chosen were of significant order. However, not in every case, all power terms were proven significant (*i.e.*, their associated fitting errors were too big for some power parameters to be considered).

RESULTS

The previously mentioned obtained polynomial functions are given collectively and as numbered equations in tab. 1.

Equations numbered in tab. 1 are interpreted in the following generic manner

$$\langle \pm\delta \rangle(x) = \sum_{i=0}^{8} B_i x^i \tag{10}$$

Table 2 presents the standard errors of parameters B_i as these resulted from the fitting procedures. Further, tab. 2 contains the Adj. R^2 coefficient of determination for all fittings.

Following eq. (10) and tabs. 1 and 2 it is easily derived that, for example, eq. (11) could be written as

$$\begin{aligned}\langle +\delta F \rangle(1/X_{tt}) &= (0.8 \pm 0.1) + \\ &+(0.30 \pm 0.03)(1/X_{tt}) - \\ &-(0.0040 \pm 0.0009)(1/X_{tt})^2 + \\ &+(3.4\cdot 10^{-5} \pm 7.3\cdot 10^{-6})(1/X_{tt})^3\end{aligned} \tag{11}$$

while, once more, for example, eq. (20) could be written as

$$\begin{aligned}\frac{\langle +\delta F \rangle}{F}(1/X_{tt}) &= (0.49 \pm 0.01) - \\ &-(0.032 \pm 0.006)(1/X_{tt}) + \\ &+(0.0013 \pm 0.0003)(1/X_{tt})^2 - \\ &-(2.1\cdot 10^{-5} \pm 0.7\cdot 10^{-5})(1/X_{tt})^3 + \\ &+(1.1\cdot 10^{-7} \pm 0.4\cdot 10^{-7})(1/X_{tt})^4\end{aligned} \tag{20}$$

It has to be mentioned that, since all equations resulted from the digital reprocessing of figs. 1 and 2, there should exist a validity region for each of the above equations. This is accounted for in tab. 3.

All fittings regarding the uncertainty of F were based on $N = 27$ pairs of digitized coordinates, while all fittings regarding the uncertainty of S were based on $N = 36$ pairs. The necessary values of F were obtained from eq. (5) and the necessary values of S from eq. (6). Obtaining F and S from the graphs in figs. 1 and 2 respectively instead of obtaining them from eqs. (5) and (6), resulted in almost identical fittings; the corresponding parameters were found to be slightly different within error. All fittings were performed using the Levenberg – Marquardt method and the commercially available software OriginPro 9.0.0 Pro (32-bit) SR2 b87 by OriginLab Corporation (http://www.OriginLab.com).

The fittings for $\langle \delta F \rangle$ present an excellent $R^2 \geq 0.97$; the fittings for $\langle \delta S \rangle$ present a very good $R^2 \geq 0.85$; the fittings for $\langle \delta F \rangle/F$ present a very good $R^2 \geq 0.77$; finally, the fittings for $\langle \delta S \rangle/S$ present a very good $R^2 \geq 0.97$.

DISCUSSION AND CONCLUSIONS

Within this study, several parametric equations in polynomial form have been prepared and presented re-

Table 1. Parameters of the polynomial functions for $\langle \pm\delta F \rangle$ and $\langle \pm\delta S \rangle$

Equation number	Function	B_0	B_1	B_2	B_3	B_4	B_5	B_6	B_7	B_8
11	$\langle +\delta F \rangle(1/X_{tt})$	0.8	0.30	–0.0040	$3.4\cdot 10^{-5}$	–	–	–	–	–
12	$\langle +\delta F \rangle(F)$	0.3	0.32	–0.005	$8\cdot 10^{-5}$	–	–	–	–	–
13	$\langle -\delta F \rangle(1/X_{tt})$			$-6\cdot 10^{-4}$	–	–	–	–	–	–
14	$\langle -\delta F \rangle(F)$		0.16	$-4\cdot 10^{-4}$	–	–	–	–	–	–
15	$\langle +\delta S \rangle(Re)$			10·9	10^{-14}	10^{-19}	–	$-1.76669\cdot 10^{-30}$	$2.31166\cdot 10^{-36}$	$-1.25773\cdot 10^{-42}$
16	$\langle +\delta S \rangle(S)$								1107	
17	$\langle -\delta S \rangle(Re)$	–0.09	$8.9\cdot 10^{-6}$	$-1.8\cdot 10^{-10}$	10^{-15}	$-7.5\cdot 10^{-21}$	$1.6\cdot 10^{-26}$	$-1.3\cdot 10^{-32}$		
18	$\langle -\delta S \rangle(S)$	–0.4	11		309		522		–	–
19	$[F^{-1}\langle +\delta F \rangle](1/X_{tt})$	0.49	–0.032		$-2.1\cdot 10^{-5}$	$1.1\cdot 10^{-7}$	–	–	–	–
20	$[F^{-1}\langle +\delta F \rangle](F)$	0.51	–0.02	0.0006	$-5\cdot 10^{-6}$	–	–	–	–	–
21	$[F^{-1}\langle -\delta F \rangle](1/X_{tt})$	0.413	–0.032		$-1.8\cdot 10^{-5}$	10^{-8}	–	–	–	–
22	$[F^{-1}\langle -\delta F \rangle](F)$	0.44	–0.028	$8\cdot 10^{-4}$	$-7\cdot 10^{-6}$	–	–	–	–	–
23	$[S^{-1}\langle +\delta S \rangle](Re)$	–1.4	$1.2\cdot 10^{-4}$	$-3.1\cdot 10^{-9}$	$4.0\cdot 10^{-14}$	10^{-19}	$1.2\cdot 10^{-24}$	$-2.9\cdot 10^{-30}$	E-36	$-2.0\cdot 10^{-42}$
24	$[S^{-1}\langle +\delta S \rangle](S)$							–	–	–
25	$[S^{-1}\langle -\delta S \rangle](Re)$	–0.25	$2.1\cdot 10^{-5}$	$-3.8\cdot 10^{-10}$	$3.195\cdot 10^{-15}$	$-1.1\cdot 10^{-20}$	$1.3\cdot 10^{-26}$	–	–	–
26	$[S^{-1}\langle -\delta S \rangle](S)$	–0.22	30.3	–289	1136.8	–2207	2092	–773	–	–

Table 2. Respective fitting errors of the parameters presented in tab. 1

Equation number	Function	B_0	B_1	B_2	B_3	B_4	B_5	B_6	B_7	B_8	R^2
11	$<+\delta F>(1/X_{tt})$	±0.1	±0.03	±0.0009	$\pm0.7\cdot10^{-5}$	–	–	–	–	–	0.99
12	$<+\delta F>(F)$	±0.1	±0.04	±0.001	$\pm2\cdot10^{-5}$	–	–	–	–	–	0.99
13	$<-\delta F>(1/X_{tt})$	CONST		$\pm1\cdot10^{-4}$	–	–	–	–	–	–	
14	$<-\delta F>(F)$	CONST	±0.01	$\pm2\cdot10^{-4}$	–	–	–	–	–	–	0.98
15	$<+\delta S>(\mathrm{Re})$	NA*	NA	NA	NA	NA	NA	NA	NA	NA	
16	$<+\delta S>(S)$	NA	NA	NA	NA	NA	NA	NA	NA	–	0.96
17	$<-\delta S>(\mathrm{Re})$	±0.02	$\pm1.2\cdot10^{-6}$	$\pm0.3\cdot10^{-10}$	CONST	$\pm1.8\cdot10^{-21}$	$\pm0.5\cdot10^{-26}$	$\pm0.5\cdot10^{-32}$	–	–	0.86
18	$<-\delta S>(S)$	±0.1	±2	CONST	±54	CONST	±100	CONST	–	–	0.87
19	$[F^{-1}<+\delta F>](1/X_{tt})$	±0.01	±0.006	CONST	$\pm0.7\cdot10^{-5}$	$\pm0.4\cdot10^{-7}$	–	–	–	–	0.78
20	$[F^{-1}<+\delta F>](F)$	±0.02	±0.004	±0.0002	$\pm2\cdot10^{-6}$	–	–	–	–	–	0.77
20	$[F^{-1}<-\delta F>](1/X_{tt})$	±0.008	±0.003	CONST	$\pm0.3\cdot10^{-5}$	$\pm2\cdot10^{-8}$	–	–	–	–	0.94
22	$[F^{-1}<-\delta F>](F)$	±0.01	±0.002	$\pm1\cdot10^{-4}$	$\pm1\cdot10^{-6}$	–	–	–	–	–	0.92
23	$[S^{-1}<+\delta S>](\mathrm{Re})$	±0.2	$\pm0.2\cdot10^{-4}$	$\pm0.4\cdot10^{-9}$	$\pm0.6\cdot10^{-14}$	CONST	$\pm0.2\cdot10^{-24}$	$\pm0.6\cdot10^{-30}$	CONST	$\pm0.5\cdot10^{-42}$	0.97
24	$[S^{-1}<+\delta S>](S)$	NA	NA	NA	NA	NA	NA	–	–	–	0.97
25	$[S^{-1}<-\delta S>](\mathrm{Re})$	±0.06	$\pm0.3\cdot10^{-5}$	$\pm0.5\cdot10^{-10}$	CONST	$\pm0.2\cdot10^{-20}$	$\pm0.2\cdot10^{-26}$	–	–	–	0.97
26	$[S^{-1}<-\delta S>](S)$	CONST	CONST	±82	CONST	±572	±549	±208	–	–	0.97

*NA: Not Applicable, the significant digits employed in the parameters of tab. 2 were more than what fitting errors indicate
CONST: Constant, respective parameter in tab. 2 was taken as constant

Table 3. Validity ranges for eqs. (11) to (26)

Equation number	Valid for
11 and 19	$1/X_{tt}$ in [0.118, 87.7]
12 and 20	F in [0.999, 63.4]
13 and 21	$1/X_{tt}$ in [0.105, 90.1]
14 and 22	F in [0.999, 63.4]
15 and 23	Re in [22290, 422616]
16 and 24	S in [0.108, 0.777]
17 and 25	Re in [18393, 321386]
18 and 26	S in [0.108, 0.777]

garding the uncertainty, in the supposed level $k = 1$, of the Reynolds number factor F and the suppression factor S used in the Chen correlation [1, 2]. These equations could be used to estimate at least a part of the uncertainty of this particular correlation, thus giving the scientific community a chance to use the correlation appropriately or even disregard it in favor of alternatives, a good summary and comparison of which could be found in [18]. The analysis resulting in these uncertainty equations reveals that the positive part of the uncertainties $<+\delta F>$ and $<+\delta S>$ is not equal to the respective negative part $<-\delta F>$ and $<-\delta S>$.; in fact, the positive part is almost always greater than the negative one.

This raises questions about the validity and applicability of eq. (8), on which the present study is largely based. This discrepancy over symmetry could be attributed not only to the actual experimental data but also to the graphical nature of the data used for all calculations. Figures 3 and 4 as well as tab. 4 summarize the statistics for the quantity $<+\delta F>/<-\delta F>$ and the quantity $<+\delta S>/<-\delta S>$. It becomes evident that both quantities are statistically different than unity. Moreover, and following figs. 3 and 4 and tab. 4, this discrepancy does not seem to be manageably close to "1".

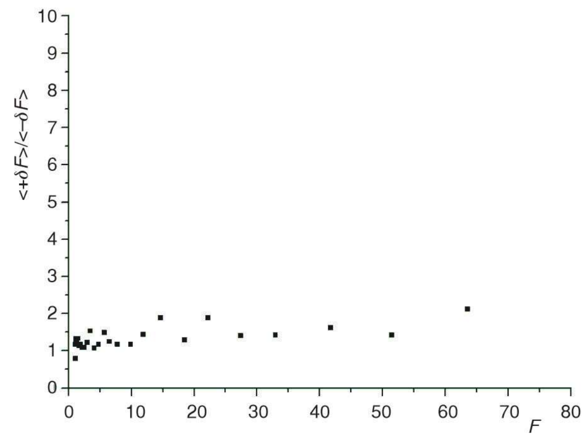

Figure 3. Ratio $<+\delta F>/<-\delta F>$ *vs*. factor F: there is an obvious but small positive discrepancy from "1"

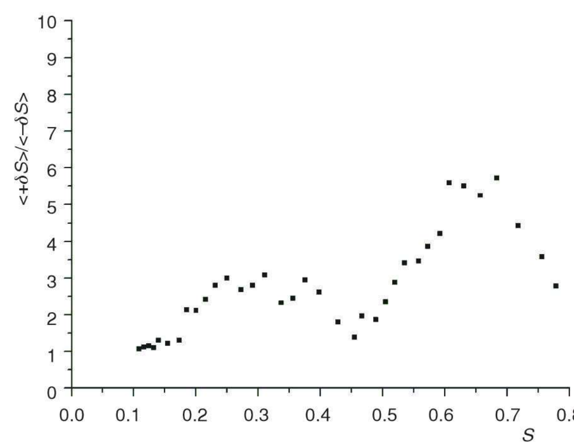

Figure 4. Ratio $<+\delta S>/<-\delta S>$ *vs*. factor S: there is an obvious and great positive discrepancy from "1"

Table 4. Statistics of <+*δF*>/<–*δF*> and <+*δS*>/<–*δS*>

	<+*δF*>/<–*δF*>	<+*δS*>/<–d*S*>
N	27	36
Mean	1.3	2.8
Std.dev	0.3	1.3
Minimum	0.8	1.1
Median	1.3	2.7
Maximum	2.1	5.7

Therefore, two options may be used: Invoke eq. (8) using the maximum of the two uncertainties, *i.e.*, in most cases, <+*δF*> and <+*δS*>. This is the most usual approach to be on the safe side and Invoke equation (8) twice, once using <+δF> and <+δS> and once using <–*δF*> and <–δ*S*>, thus resulting in an estimated uncertainty range.

The parametric equations for <*δF*> are given once as a function of $1/X_{tt}$ and once as a function of F, to provide room for implementations originating from different viewpoints. The same applies to the <*δS*> equations, which are provided as functions of Reynolds number or *S*. For those interested in the relative uncertainty the authors of this work provide a set of respective equations, as in the previous section.

Due to the nature of figs. 1 and 2 being *log-log* and *log-linear* respectively, and due to the digitization process, the research team doubled-checked the fitting results visually, so that deviations not obvious in the numerical results could be verified independently. This process resulted that not all fitting parameters could be considered within error. Some should be taken as constants (CONST, *i.e.*, *constant*, in tab. 2) or with more significant digits than their standard error dictates (NA, *i.e.*, *Not Applicable*, in tab. 2).

It becomes evident from relative uncertainties that the largest part of the Chen correlation uncertainty attributed to factors *F* and *S* is due to the uncertainty of factor *S*. Figure 5 gives a visual representation of this conclusion. Therefore, and given the square power in eq. (8) one could consider only the <+*δS*> component of the uncertainty for factors *F* and *S* and still be close to the maximum safe side as in first comment.

Figures 6 to 9 give a visual representation of the quality of the <+*δF*> and <+*δS*> uncertainties calculations using equations (12), (13), (16), (17), (20), (21), (24) and (25). The <–*δF*> and <–*δS*> uncertainties equations were not considered since they are considerably smaller and not on the safe side. In detail:

Figure 6 presents, against data, the worst of the function fitting (yet, still, very good) for <+*δF*> and particularly for eq. (21).

Figure 7 presents, against data, the second worst of the function fittings for eq. (16).

Figure 8 presents in actual fig. 1, the function fitting of eq. (13) as being one of the best.

Finally and similarly, fig. 9 presents in actual fig. 2, the function fitting of eq. (25), once more as being one of the best.

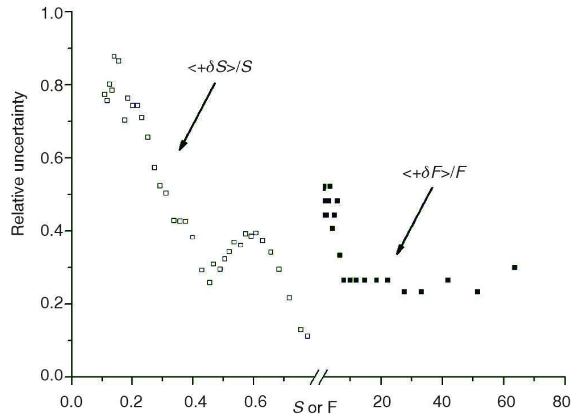

Figure 5. Relative uncertainty <+*δS*>/*S* is in most cases significantly greater than relative uncertainty <+*δF*>/*F*

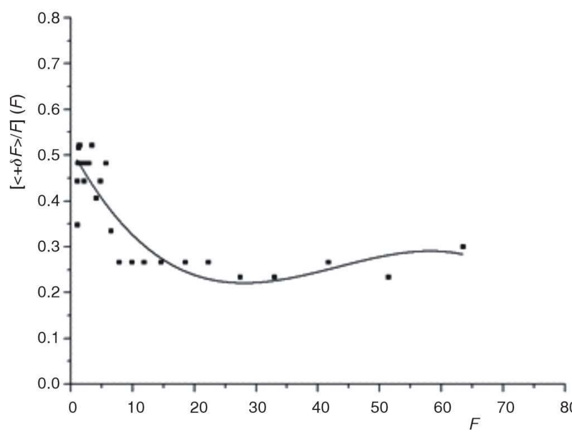

Figure 6. Line of eq. (20) *vs*. actual data collected from fig. 1. Worst R^2 equal to 0.77

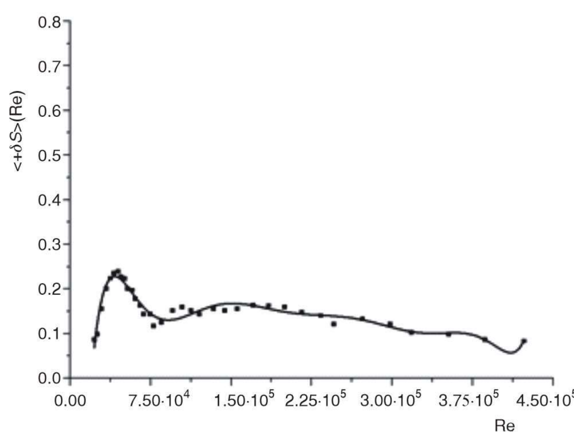

Figure 7. Line of eq. (15) *vs*. actual data collected from fig. 2. Second worse R^2 equal to 0.91

Overall, and without any hesitation, it could be argued that the uncertainties found for the Chen correlation for the boiling heat transfer coefficient at saturated flow [1, 2] agree well with the discrepancies found for this very correlation against experimental data, as thoroughly reported in [18].

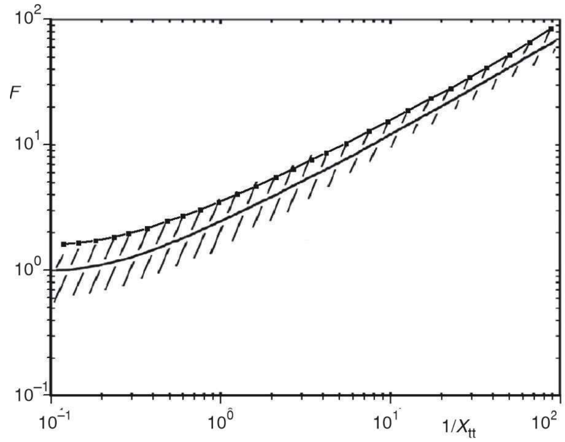

Figure 8. Line of eq. (12) on the actual graph of fig. 1. R^2 equal to 0.99

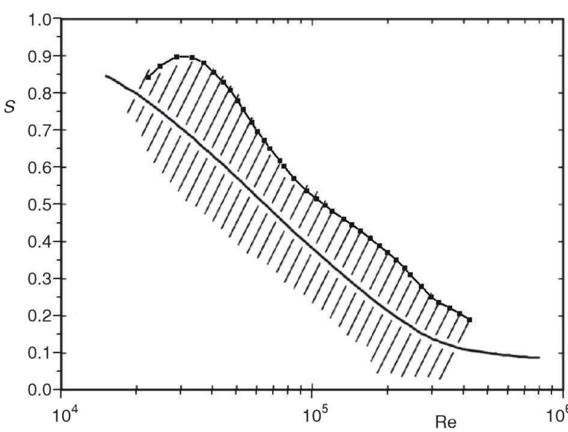

Figure 9. Line of eq. (24) on the actual graph of fig. 2. R^2 is equal to 0.97

REFERENCES

[1] Chen, J. C., *A Correlation for Boiling Heat Transfer to Saturated Fluids in Convective Flow*, ASME Publication, 1963, pp. 2-6, 63-HT-34

[2] Chen, J. C., Correlation for Boiling Heat Transfer to Saturated Fluids in Convective Flow, *Ind. Eng. Chem. Process Des. Dev. 5* (1966), (3), pp. 322-329

[3] Dittus, F. W., Boelter, L. M. K., *Heat Transfer in Automobile Radiators of the Tubular Type*, vol. 2. University of California Publications in Engineering, Berkeley, 1930, pp. 443-461

[4] Forster, H. K., Zuber, N., Dynamics of Vapor Bubbles and Boiling Heat Transfer, *AIChE J. 1* (1955), 4, pp. 531-535

[5] Chen, W., Fang, X., A Note on the Chen Correlation of Saturated Flow Boiling Heat Transfer, *International Journal of Refrigeration, 48* (2014), Dec., pp. 100-104

[6] Collier, J. G., Forced Convection Boiling, in: (Bergles, A. E., *et al*., Eds.), *Two-phase Flow and Heat Transfer in the Power and Process Industries*, Hemisphere Publishing Corp., Washington, D. C., 1981, Chap. 8

[7] Groeneveld, D. C., Snoek, C. W., A Comprehensive Examination of Heat Transfer Correlations Suitable for Reactor Safety Analysis, in Multiphase Science and Technology (Eds. Hewitt, G. F., *et al*.), 2, pp. 181-274, 1986 Springer

[8] Kreith, F., Bohn, M. S., *Principles of Heat Transfer*, 4th ed. Harper & Row, Publishers, New York, USA, 1986

[9] Yu, W., *et al*., Two-Phase Pressure Drop, Boiling Heat Transfer, and Critical Heat Flux to Water in a Small-Diameter Horizontal Tube, *Int. J. Multiph. Flow, 28* (2002), 6, pp. 927-941

[10] Zhang, W., *et al*., Correlation for Flow Boiling Heat Transfer in Mini-Channels, *Int. J. Heat Mass Transf. 47* (2004), Dec., pp. 5749-5763

[11] Steiner, H., *et al*., A Wall Heat Transfer Model for Subcooled Boiling Flow, *Int. J. Heat. Mass Transf. 48* (2005), 19, pp. 4161-4173

[12] Zhang, W., *et al*., Correlation for Flow Boiling Heat Transfer at Low Liquid Reynolds Number in Small Diameter Channels, *J. Heat. Transf., 127* (2005), 11, pp. 1214-1221

[13] Kolev, N. I., *Multiphase Flow Dynamic 2: Thermal and Mechanical Interactions*, 3rd ed. Springer Verlag, Berlin, 2007

[14] Vashisth, S., *et al*., A Review on the Potential Applications of Curved Geometries in Process Industry, *Ind. Eng. Chem. Res., 47* (2008), 10, pp. 3291-3337

[15] Orian, G., *et al*., Flow Boiling of Binary Solution in Horizontal Tube, *Energy, 35* (2010), 1, pp. 35-44

[16] Fang, X. D., *et al*., Review of Correlations of Flow Boiling Heat Transfer Coefficients for Carbon Dioxide, *Int. J. Refrigeration, 36* (2013), Dec., pp. 2017-2039

[17] ***, ISO/IEC Guide 98-3:2008, Uncertainty of Measurement – Part 3: Guide to the Expression of Uncertainty in Measurement (GUM:1995)

[18] ElFaham, M., Tang, C. C., A Comparative Analysis of Two-Phase Flow Boiling Heat Transfer Coefficient and Correlations for Hydrocarbons and Ethanol, *Energies 16* (2023), 5931

Received on June 20, 2024
Accepted on August 23, 2024

Електра Д. ПУЛОПУЛУ, Ник П. ПЕТРОПУЛОС

ТЕХНИЧКА БЕЛЕШКА О НЕОДРЕЂЕНОСТИ ЧЕНОВЕ КОРЕЛАЦИЈЕ ЗА КОЕФИЦИЈЕНТ ПРЕНОСА ТОПЛОТЕ КЉУЧАЊА ПРИ ЗАСИЋЕНОМ ПРОТОКУ

Такозвана *Ченова корелација* за коефицијент преноса топлоте кључања при засићеном протоку од објављивања 1966. године, углавном се наводи као једна од најуспешнијих те врсте. Као што је познато, заснива се на сабирању чланова који се односе на пренос топлоте у течном делу и пренос топлоте у парном делу. Одговарајуће формуле укључују и Рејнолдсов фактор F и фактор потиска S. У то време, Чен је прихватио да се F и S изведу графички. Ипак, и углавном у рачунске сврхе, предложено је неколико једначина које апроксимирају ова два фактора. Ове једначине су проверене на тачност и грешке у куцању и сада су широко прихваћене. Међутим, није било покушаја да се резултати Ченове корелације повежу са очекиваном неодређеношћу. Циљ овог кратког извештаја је да се обради Ченова корелација у смислу њене несигурности засноване на неизвесности фактора F и S. Неодређености F и S изведене су дигитално из графика F и S у оригиналном раду Чена из 1966. године. Након дигитализације подаци о неодређености обрађени су да би се добиле формуле неодређености у полиномијалном облику. Прихваћено је да је ниво неодређености Ф и S, $\kappa = 1$.

Кључне речи: Ченова корелација, проток кључања при засићењу, коефицијент преноса топлоте, Рејнолдсов фактор, фактор потиска